Bone Microarchitecture and Stiffness in Premenopausal Women with Idiopathic Osteoporosis

Adi Cohen, X. Sherry Liu, Emily M. Stein, Donald J. McMahon, Halley F. Rogers, Jeanette LeMaster, Robert R. Recker, Joan M. Lappe, X. Edward Guo, and Elizabeth Shane

Department of Medicine (A.C., E.M.S., D.J.M., H.F.R., E.S.) and Bone Bioengineering Laboratory, Department of Biomedical Engineering (X.S.L., X.E.G.), Columbia University, New York, New York 10032; and Creighton University (J.L., R.R.R., J.M.L.), Omaha, Nebraska 68131

Context: Idiopathic osteoporosis (IOP) is an uncommon disorder in which low areal bone mineral density (aBMD) and/or fractures occur in otherwise healthy premenopausal women.

Objectives: Our objectives were to characterize bone mass, microarchitecture, and trabecular bone stiffness in premenopausal IOP and to determine whether women with low aBMD who have never fractured have abnormal microarchitecture and stiffness.

Design, Setting, and Patients: We conducted a prospective cohort study of 27 normal controls and 31 women with IOP defined by low trauma fracture (n = 21) or low BMD (Z score ≤ -2.0; n = 10).

Main Outcome Measures: We assessed aBMD by dual-energy x-ray absorptiometry; volumetric BMD and cortical and trabecular microarchitecture of the radius and tibia by high-resolution (82 μm) peripheral quantitative computed tomography; and trabecular bone stiffness (elastic moduli), estimated by micro-finite element analysis.

Results: Fracture subjects did not differ from controls by age or body mass index, which was lower in low-BMD subjects than controls. Fracture subjects also had lower aBMD than controls at all sites ($P < 0.05$–0.0001). Bone size was similar in controls and fracture subjects but 10.6% smaller in low-BMD subjects ($P < 0.05$). Every trabecular parameter in both fracture and low-BMD groups was markedly worse than controls ($P < 0.01$–0.0001). Cortical thickness was significantly lower in both fracture and low-BMD groups at the tibia but not radius. Bone stiffness estimated by micro-finite element analysis was comparably reduced in low-BMD and fracture groups.

Conclusion: Premenopausal women with IOP had marked trabecular microarchitectural deterioration at the radius and tibia. Cortical parameters were affected only at the tibia. Although they had not fractured, microarchitectural deterioration was similar in IOP women with low BMD and those with fractures. **(*J Clin Endocrinol Metab* 94: 4351–4360, 2009)**

In postmenopausal women, low bone mineral density (BMD) and fragility fractures are common, and measurement of areal BMD (aBMD) by dual-energy x-ray absorptiometry (DXA) is an excellent tool for prediction of future fractures (1). Quantitative histomorphometry of transiliac bone biopsies has demonstrated that microarchitectural deterioration generally underlies low BMD measurements in postmenopausal women (2–4).

In premenopausal women, low aBMD and fractures are uncommon (5, 6), and the relationship of low aBMD measurements and fractures to bone microarchitecture, strength, and future fracture have not been defined (7, 8).

ISSN Print 0021-972X ISSN Online 1945-7197
Printed in U.S.A.

doi: 10.1210/jc.2009-0996 Received May 12, 2009. Accepted August 10, 2009.
First Published Online October 16, 2009.

Abbreviations: aBMD, Areal bone mineral density; BMI, body mass index; BV, bone volume; 3D, three-dimensional; D_{trab}, trabecular bone density; DXA, dual-energy x-ray absorptiometry; μFE, micro-finite element; HA, hydroxyapatite; HR-pQCT, High-resolution peripheral quantitative computed tomography; IOP, idiopathic osteoporosis; Tb.N, trabecular number; Tb.Sp, trabecular separation; Tb.Th, trabecular thickness; TV, total volume; vBMD, volumetric BMD; VOI, volume of interest.

In otherwise healthy young women, low aBMD measurements may be an artifact of small bone size (9, 10) or due to genetically determined low peak bone mass (11); bone microarchitecture and strength may be normal and short-term fracture risk very low. Conversely, low aBMD may be due to premature bone loss with microarchitectural deterioration, and short-term risk of fractures may be higher. Although low trauma fractures in young women should raise concerns for bone health, they have not been definitively linked to abnormal bone microarchitecture. One retrospective bone biopsy study of young adults with unexplained fractures found abnormal cancellous and cortical microarchitecture (12), whereas another did not (13).

High-resolution peripheral quantitative computed tomography (HR-pQCT) (Xtreme CT; Scanco Medical AG, Bassersdorf, Switzerland) of the distal radius and tibia is a new, noninvasive, three-dimensional (3D) imaging technique that provides a true volumetric measurement of BMD (vBMD). Its resolution is sufficiently high (voxel size = 82 μm) to distinguish between cortical and cancellous bone and to visualize fine details of trabecular microarchitecture that were previously measureable only on bone biopsies. In postmenopausal women with fractures, HR-pQCT revealed cortical thinning and decreased cancellous bone volume, with fewer, more widely spaced trabeculae and increased heterogeneity of the trabecular network (14–16). Micro-finite element (μFE) analysis techniques applied to HR-pQCT data sets provide an estimate of bone mechanical competence (stiffness) that distinguishes between groups of subjects with and without fractures (17, 18).

In this study, we used HR-pQCT and μFE techniques to characterize cortical and cancellous vBMD, trabecular microarchitecture, and trabecular bone mechanical competence in otherwise healthy premenopausal women with idiopathic osteoporosis (IOP), defined as low trauma fractures and/or low aBMD by DXA, with no historical or biochemical secondary cause of osteoporosis. We hypothesized that, despite their relative youth, young women with low trauma fractures have microarchitectural deterioration and detectable reductions in estimated bone stiffness (strength). Conversely, we anticipated that young women with low aBMD measurements who had not had a fracture would have normal microarchitecture.

Patients and Methods

Patient population

Premenopausal women, aged 18–48 yr, were recruited at Columbia University (New York, NY) and Creighton University (Omaha, NE) by advertisement, self-referral, or physician referral. Subjects were eligible for inclusion if there was a documented history of low-trauma fractures after age 18 or very low aBMD by DXA (T score ≤ -2.5 or Z score ≤ -2.0) at the spine or proximal femur. Low trauma was defined as equivalent to a fall from a standing height or less, excluding skull or digit fractures. Fractures were ascertained by review of radiographs or radiograph report. To qualify as normal controls, women were required to have normal aBMD by DXA (T score ≥ -1.0 or Z score ≥ -1.0) and no history of low-trauma fractures. Premenopausal status was defined by regular menstrual cycles off hormonal contraception and early follicular-phase FSH levels lower than 20 mIU/ml. Subjects and controls were excluded if they had given birth or had lactated within the past 12 months. Cases and controls had a detailed history and physical and biochemical evaluation to exclude secondary causes of osteoporosis, including disorders causing premenopausal estrogen deficiency, endocrinopathies (*e.g.* hyperthyroidism, Cushing's syndrome, or prolactinoma), anorexia nervosa, bulimia, celiac or other gastrointestinal diseases, abnormal mineral metabolism (*e.g.* osteomalacia or hyperparathyroidism), hypercalciuria (>300 mg/g creatinine), and drug exposures (*e.g.* glucocorticoids, anticonvulsants, anticoagulants, or methotrexate). Women with serum 25-hydroxyvitamin D (25-OHD) levels lower than 10 ng/ml were excluded. Because vitamin D deficiency and insufficiency are common and commercial assays variable, women with 25-OHD levels between 10 and 20 ng/ml were enrolled if their serum PTH was normal (10–65 pg/ml).

All subjects provided written informed consent, and the Institutional Review Boards of both institutions approved these studies.

Laboratory assessments

Fasting morning blood was drawn during the early follicular phase of the menstrual cycle and analyzed as convenience samples in a clinical laboratory for complete blood count, erythrocyte sedimentation rate, serum electrolytes, renal and hepatic function, FSH, celiac antibodies (tissue transglutaminase, endomysial), protein electrophoresis, thyroid function, PTH, and 25-OHD; 24-h urine collections were analyzed for free cortisol, calcium, and creatinine. Serum and urine were archived and stored at −80 C for batch analyses in research laboratories when recruitment is complete.

aBMD

aBMD was measured by DXA (QDR-4500; Hologic Inc., Walton, MA) at Columbia and Creighton University Medical Centers. T and Z scores compared subjects and controls with young normal and age-matched populations of the same race and sex, as provided by the manufacturer. Scanners at both sites were cross-calibrated with a reference phantom to read BMD within 1% at baseline and at 6-month intervals throughout the study.

HR-pQCT of the radius and tibia

HR-pQCT (XtremeCT; Scanco Medical AG) was performed at Columbia University in all participants, including those recruited at Creighton University. The nondominant forearm and distal tibia were immobilized in a carbon fiber shell and scanned as described (14, 15, 17). The region of interest is defined on a scout film by manual placement of a reference line at the endplate of the radius or tibia; the first slice is 9.5 and 22.5 mm proximal to the reference line at the radius and tibia, respectively (Fig. 1A).

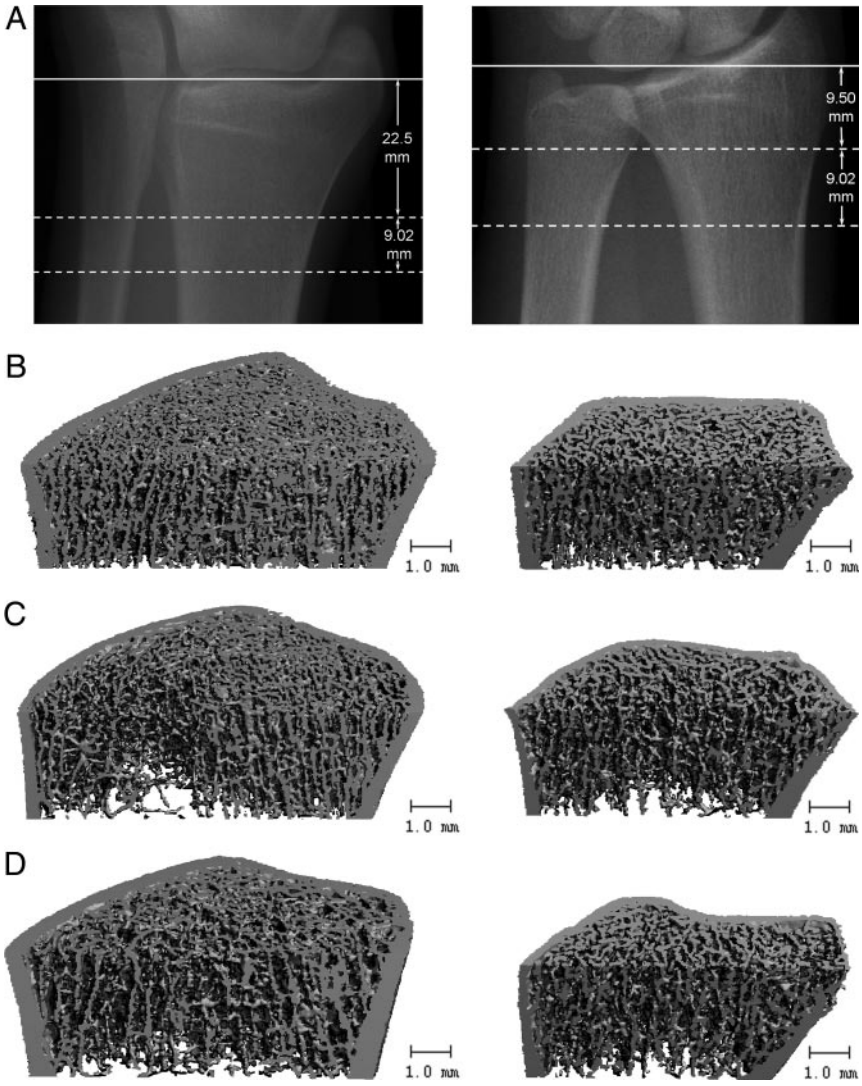

FIG. 1. A, HR-pQCT scout films of the tibia (*left*) and radius (*right*) illustrating the placement of the reference line at the endplate of the tibia or radius. The first slice of the region of interest is 22.5 and 9.5 mm proximal to the reference line at the tibia and radius, respectively. A stack of 110 parallel CT slices provides a 3D image of approximately 9 mm in the axial direction (*dashed lines*). B–D, Representative HR-pQCT scans from control (B), fracture (C), and low-BMD (D) subjects.

A stack of 110 parallel CT slices is acquired at the distal end of both sites using an effective energy of 40 keV, slice thickness of 82 μm, image matrix size 1024 × 1024, with a nominal voxel size of 82 μm. This provides a 3D image of approximately 9 mm in the axial direction. Attenuation data are converted to equivalent hydroxyapatite (HA) densities. The European Forearm Phantom is scanned regularly for quality control.

The analysis methods have been described, validated (19–22), and applied in several recent clinical studies (14, 15, 17, 18, 23, 24). Briefly, the volume of interest (VOI) is automatically separated into cortical and trabecular regions using a threshold-based algorithm set to one third the apparent cortical bone density. Mean cortical thickness is defined as the mean cortical volume divided by the outer bone surface. Trabecular bone density (D_{trab}) is the average bone density within the trabecular VOI. Bone volume (BV)/total volume (TV) (percent) is derived from D_{trab} assuming the density of fully mineralized bone is 1200 mg HA/cm^3 (BV/TV = 100 × D_{trab}/1200 mg HA/cm^3). Measurements of trabecular microstructure are limited by the resolution of the XtremeCT, which approximates the width of individual trabeculae. Therefore, trabecular structure is assessed using a semi-derived algorithm (20, 25). Trabeculae are identified by a mid-axis transformation method and the distance between them assessed by the distance-transform method (26). Trabecular number (Tb.N) is the inverse of the mean spacing of the mid-axes. Trabecular thickness (Tb.Th) and trabecular separation (Tb.Sp) are then derived from BV/TV and Tb.N using formulae from traditional quantitative histomorphometry; Tb.Th = (BV/TV)/Tb.N and Tb.Sp = (1 − BV/TV)/Tb.N.

μFE analysis based on HR-pQCT images

We used HR-pQCT data to calculate apparent anisotropic elastic moduli of trabecular bone, a surrogate measure of bone's resistance to force, otherwise termed mechanical competence or stiffness. First, the mineralized phase was thresholded automatically by using a Laplace-Hamming filter followed by global threshold using a fixed value of 40% of maximal grayscale value of the images (27). Then a VOI of 70 × 70 × 70 voxels, corresponding to 5.74 × 5.74 × 5.74 mm^3, was isolated manually from the center of each thresholded radius image, and a VOI of 110 × 110 × 110 voxels, corresponding to 9.02 × 9.02 × 9.02 mm^3, was isolated manually from the center of each thresholded tibia image. The location of the VOI was defined by the center of the largest cylinder that could fit within the trabecular compartment, providing a reproducible location based on a customized protocol. Each subvolume of the HR-pQCT image of the distal radius and distal tibia was converted to a μFE model by directly converting bone voxels to eight-node elastic brick elements with an element size of 82 × 82 × 82 μm^3. Bone tissue properties were assumed to be isotropic and linearly elastic with a Young's modulus of 15 GPa and a Poisson's ratio of 0.3 for all models (28). Three μFE analyses, representing three uniaxial compressions, were performed on each model using an element-by-element preconditioned conjugate gradient solver (29–31). Based on the anisotropic compliance matrix, estimated apparent elastic constants (three apparent Young's moduli, E_{11}, E_{22}, and E_{33}) were calculated and sorted. E_{11} represents the modulus along the medial-lateral direction, E_{22} along the anterior-posterior direction, and E_{33} along the axial direction.

Statistical analysis

Statistical analyses were performed using SAS software (SAS Institute, Cary, NC). ANOVA was used to examine overall differences among the three groups (controls, fracture, and low-

BMD). Between-groups comparisons were conducted using Student's *t* tests. Logistic regression analyses were used to control for covariates. All data are expressed as mean ± SD.

Results

Characteristics of the study population

The study population comprised 27 controls and 31 subjects with IOP, 21 included because of low trauma adult fractures whether or not they had low aBMD (fracture group) and 10 with low aBMD but no adult low trauma fractures (low-BMD group). In the fracture group, the number of fractures ranged from one to 12. Eleven subjects had multiple (two to 12) fractures; two had vertebral, three had hip, nine had rib, nine had arm or forearm, and seven had ankle or metatarsal fractures. BMD was in the osteoporotic range (T score ≤ -2.5 or Z score ≤ -2.0) in nine fracture subjects (43%).

Mean age, height, weight, body mass index (BMI), and BMD are presented in Table 1. Controls had slightly higher weight and BMI than IOP subjects, although the difference did not reach statistical significance. However, within the IOP group, low-BMD subjects were shorter and weighed significantly less than controls, whereas fracture subjects did not differ from controls.

A family history of osteoporosis, reported in 52% of controls and 65% of IOP subjects (*P* value nonsignificant), was more common in the low-BMD group than in the fracture group (90 *vs.* 52%; $P = 0.04$).

aBMD was lower at all sites in IOP subjects than controls (Table 1). Within the IOP group, mean aBMD of the IOP fracture group was within the expected range for age (Z score ≥ -2.0) at all sites. Despite this and although they had not been selected by BMD criteria, the IOP fracture group had significantly lower aBMD at all sites than controls. Differences in BMD remained significant after controlling for BMI.

Selected laboratory results from the initial evaluation to exclude secondary causes of osteoporosis (Table 1) revealed no major differences among the groups. Mean serum 25-OHD levels were similar in controls and both groups of IOP subjects. Serum 25-OHD levels below 20 ng/ml were found in a similar number of IOP subjects (n = 4; 13%) and controls (n = 3; 11%). All subjects had serum

TABLE 1. Characteristics of the study population

			IOP subgroups	
	Control, n = 27	**IOP, n = 31**	**IOP fracture, n = 21**	**IOP low BMD, n = 10**
Demographic and anthropomorphic features				
Age (yr)	34.3 ± 8.7	37.8 ± 7.7	37.1 ± 8.1	39.5 ± 6.7
Race (% Caucasian)	96	100	100	100
Height (cm)	164.1 ± 7.9	162.8 ± 6.6	163.8 ± 6.8	160.7 ± 5.9
Weight (kg)	67.7 ± 14.2	61.2 ± 16.2	64.1 ± 17.9	55.3 ± 10.2[h]
BMI (kg/m^2)	25.1 ± 4.6	23.0 ± 5.4	23.8 ± 6.0	21.4 ± 3.9[h]
BMD				
Absolute BMD (g/cm^2)				
Lumbar spine	1.093 ± 0.09	0.865 ± 0.12[c]	0.905 ± 0.13[g]	0.781 ± 0.04[i,j]
Total hip	0.969 ± 0.08	0.789 ± 0.15[c]	0.811 ± 0.17[f]	0.746 ± 0.11[i]
Femoral neck	0.850 ± 0.08	0.672 ± 0.14[c]	0.692 ± 0.15[f]	0.632 ± 0.11[i]
Distal radius	0.724 ± 0.05	0.687 ± 0.05[b]	0.691 ± 0.69[d]	0.679 ± 0.05[h]
Z score				
Lumbar spine	0.61 ± 0.82	−1.42 ± 1.16[c]	−1.06 ± 1.23[g]	−2.17 ± 0.45[i,j]
Total hip	0.28 ± 0.63	−1.00 ± 1.30[c]	−0.78 ± 1.44[e]	−1.44 ± 0.87[i]
Femoral neck	0.12 ± 0.75	−1.35 ± 1.22[c]	−1.19 ± 1.34[f]	−1.67 ± 0.92[i]
Distal radius	0.71 ± 0.80	0.18 ± 0.82[a]	0.25 ± 0.82	0.03 ± 0.83[h]
Serum and urine biochemistries				
Serum calcium (mg/dl)	9.1 ± 0.2	9.0 ± 0.3	9.0 ± 0.3	9.0 ± 0.3
Serum phosphorus (mg/dl)	3.6 ± 0.4	3.4 ± 0.4	3.3 ± 0.4[d]	3.5 ± 0.5
Serum PTH (pg/ml)	34.1 ± 10.6	33.5 ± 12.3	35.5 ± 11.7	29.5 ± 13.2
Serum 25-OHD (ng/ml)	29.3 ± 9.9	34.5 ± 15.0	35.2 ± 17.1	32.9 ± 9.8
Urine calcium (mg/gCr)	134 ± 69	141 ± 56	134 ± 61	158 ± 42

Serum calcium levels are albumin-corrected measurements.

[a–c] Control *vs. IOP:* [a] $P \leq 0.05$; [b] $P \leq 0.01$; [c] $P \leq 0.0001$.

[d–g] Control *vs. IOP fracture:* [d] $P \leq 0.05$; [e] $P \leq 0.01$; [f] $P \leq 0.001$; [g] $P \leq 0.0001$.

[h–i] Control *vs. IOP low BMD:* [h] $P \leq 0.05$; [i] $P \leq 0.0001$.

[j] IOP fracture *vs.* low BMD: $P \leq 0.001$.

TABLE 2. Volumetric density, trabecular and cortical microarchitecture, and mechanical competence of the study population

			IOP subgroups	
	Control, n = 27	IOP, n = 31	IOP fracture, n = 21	IOP low BMD, n = 10
Radius				
Mean area (mm^2)	255.9 ± 30.3	236.0 ± 46.3	239.5 ± 46.7	228.7 ± 47.1[h]
Total density (mg HA/cm^3)	331.8 ± 55.2	291.5 ± 70.5[a]	297.4 ± 74.9	279.1 ± 62.2[h]
Cortical density (mg HA/cm^3)	905.8 ± 60.3	894.8 ± 86.3	891.8 ± 99.8	901.0 ± 51.5
Cortical thickness (mm)	0.814 ± 0.17	0.73 ± 0.20	0.736 ± 0.23	0.716 ± 0.13
D_{trab} (mgHA/cm^3)	158.0 ± 27.6	117.6 ± 36.4[d]	123.5 ± 38.1[g]	105.1 ± 30.6[k]
Tb.N (1/mm)	2.01 ± 0.23	1.70 ± 0.28[d]	1.73 ± 0.29[g]	1.63 ± 0.26[j]
Tb.Th (mm)	0.066 ± 0.01	0.057 ± 0.011[b]	0.059 ± 0.01[e]	0.053 ± 0.01[j]
Tb.Sp (mm)	0.440 ± 0.07	0.550 ± 0.12[d]	0.538 ± 0.12[f]	0.575 ± 0.12[k]
SD of 1/Tb.N (inhomogeneity)	0.173 ± 0.03	0.240 ± 0.07[d]	0.236 ± 0.08[f]	0.250 ± 0.06[i]
Elastic moduli (MPa)				
E_{11} (anterior-posterior)	376 ± 136	219.8 ± 162.0[c]	244 ± 179[f]	168 ± 108[k]
E_{22} (medial-lateral)	588 ± 249	356.5 ± 272.6[b]	404 ± 308[e]	257 ± 141[j]
E_{33} (longitudinal)	1160 ± 486	668.8 ± 524.7[c]	775 ± 589[e]	445 ± 254[k]
Tibia				
Mean area (mm^2)	664.2 ± 86.1	624.0 ± 89.8	638.3 ± 87.8	595.4 ± 91.5[h]
Total density (mg HA/cm^3)	303.9 ± 37.9	249.7 ± 49.4[d]	251.3 ± 54.0[g]	246.5 ± 41.2[j]
Cortical density (mg HA/cm^3)	922.8 ± 32.0	892.8 ± 47.5[b]	894.0 ± 47.1[e]	890.4 ± 50.9[h]
Cortical thickness (mm)	1.208 ± 0.16	1.00 ± 0.21[c]	1.004 ± 0.217[g]	0.998 ± 0.21[i]
D_{trab} (mg HA/cm^3)	159.5 ± 24.9	122.5 ± 37.3[d]	125.9 ± 42.9[f]	115.7 ± 22.9[k]
Tb.N (1/mm)	1.96 ± 0.28	1.56 ± 0.33[d]	1.60 ± 0.40[g]	1.49 ± 0.12[k]
Tb.Th (mm)	0.068 ± 0.010	0.065 ± 0.013	0.065 ± 0.01	0.065 ± 0.01
Tb.Sp (mm)	0.451 ± 0.07	0.605 ± 0.15[d]	0.602 ± 0.18[g]	0.610 ± 0.06[k]
SD of 1/Tb.N (inhomogeneity)	0.197 ± 0.04	0.291 ± 0.11[c]	0.297 ± 0.13[f]	0.277 ± 0.04[k]
Elastic moduli (MPa)				
E_{11} (anterior-posterior)	247.6 ± 118.3	146 ± 99[c]	155.4 ± 114.2[e]	128.7 ± 61.8[j]
E_{22} (medial-lateral)	350.7 ± 144.9	214 ± 161[b]	231.5 ± 190.1[e]	180.1 ± 77.3[k]
E_{33} (longitudinal)	943.0 ± 314.3	684 ± 414[a]	710.5 ± 488.9	633.5 ± 226.9[i]

[a–d] Control *vs. IOP:* [a] $P \leq 0.05$; [b] $P \leq 0.01$; [c] $P \leq 0.001$; [d] $P \leq 0.0001$.

[e–g] Control *vs. IOP fracture:* [e] $P \leq 0.05$; [f] $P \leq 0.01$; [g] $P \leq 0.001$.

[h–k] Control *vs. IOP low BMD:* [h] $P \leq 0.05$; [i] $P \leq 0.01$; [j] $P \leq 0.001$; [k] $P \leq 0.0001$.

PTH levels within the normal range. Among those with serum 25-OHD below 20 ng/ml, the mean PTH level was 42 ± 10 pg/ml.

HR-pQCT and μFE results in IOP and control subjects

HR-pQCT and μFE measurements are presented in Table 2. We first evaluated differences between control and both groups of IOP subjects, considered together. At the radius, there were significant differences in total vBMD (cortical plus trabecular) and all trabecular density and structural indices. IOP subjects had 12% lower total vBMD ($P = 0.02$) and 26% lower trabecular vBMD ($P < 0.0001$), 15% lower Tb.N ($P < 0.0001$), 14% lower Tb.Th ($P = 0.003$), 25% higher Tb.Sp ($P < 0.0001$), and 41% higher variability (SD) in Tb.Sp ($P < 0.0001$). Bone size (bone area) and cortical thickness tended to be lower in IOP subjects ($P = 0.06–0.09$). At the tibia, total bone vBMD, trabecular vBMD, and all structural indices except Tb.Th differed significantly. IOP subjects had 18% lower total vBMD, 23% lower trabecular vBMD, 20% lower Tb.N, 33% higher Tb.Sp, and 45% higher variability (SD) in Tb.Sp (all $P \leq 0.0001$). Bone size (mean area) tended to be lower in IOP subjects ($P = 0.09$). Cortical density and thickness were significantly lower at the tibia in IOP subjects ($P = 0.007–0.0002$). Young's moduli were substantially and significantly lower in IOP subjects than controls in all three directions at both radius and tibia (Table 2).

Figure 1, B–D, illustrates representative HR-pQCT scans from control, fracture, and low-BMD subjects. Considering low-BMD and fracture groups separately (Table 2), bone size (mean area) did not differ between control and fracture subjects, whereas the low-BMD group had significantly smaller bones than controls (Fig. 2A). Radius cortical density and thickness (Fig. 2B) did not differ between controls and either fracture or low-BMD. In contrast, tibial cortical parameters were significantly and comparably lower than controls in both fracture and low-BMD groups.

ANOVA models showed significant overall differences among the three groups for the variables of primary interest: trabecular microstructure and μFE (stiffness) indices. Virtually every trabecular parameter in both fracture

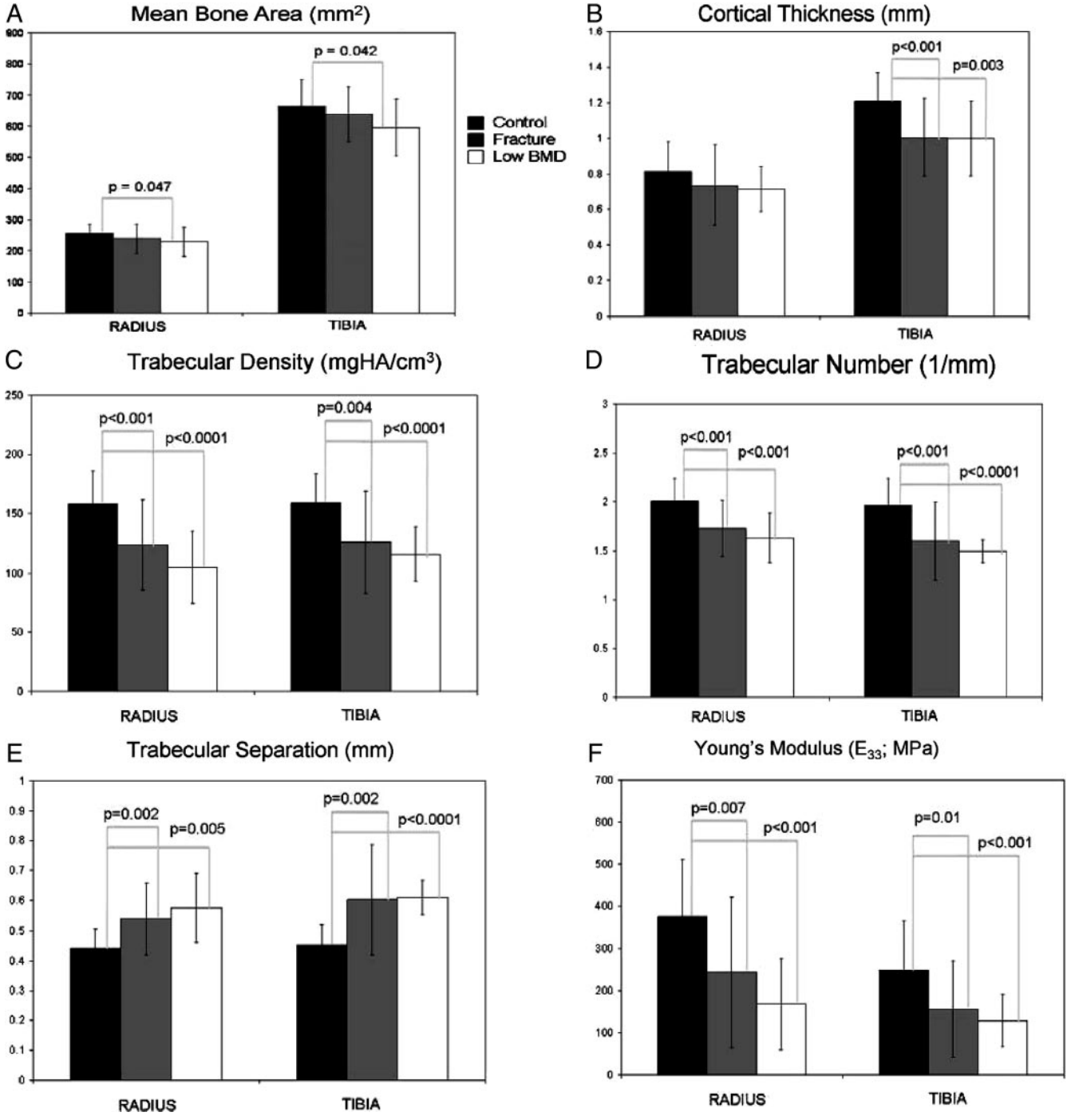

FIG. 2. Comparisons between the IOP fracture and low-BMD groups in comparison with controls for HR-pQCT variables assessed at the radius and tibia.

and low-BMD groups differed from controls. Notably, although they had not fractured, women in the low-BMD group had microarchitectural deterioration as profound as women in the fracture group (Table 3 and Fig. 2, C–E). Moreover, estimated trabecular bone stiffness was as low as or lower in the low-BMD than the fracture group (Table 2 and Fig. 2F).

Because age and BMI, PTH, and vitamin D may affect bone structure and stiffness, we compared controls and IOP, controlling for these variables. Between-groups differences in trabecular and cortical microarchitectural parameters and Young's moduli remained significant after controlling for age, BMI, PTH, and 25-OHD (data not shown).

Fracture number did not correlate with any radius HR-pQCT parameter. However, at the tibia, near-significant relationships were found between number of adult fractures and cortical density ($R = -0.244$; $P = 0.07$), Tb.N

(R = −0.242; $P = 0.07$), Tb.Sp (R = 0.245; $P = 0.07$), and Tb.Sp SD (R = 0.233; $P = 0.08$).

Discussion

To our knowledge, this is the first study to examine 3D HR-pQCT measures of bone mass, structure, and microarchitecture and μFE of HR-pQCT images to estimate trabecular bone stiffness in premenopausal women with IOP. We found that premenopausal women with IOP have significant trabecular microarchitectural deterioration compared with normal controls. Cortical density and thickness were also lower in IOP subjects, but the differences achieved statistical significance only at the tibia. In general, trabecular structure was more severely affected than cortical structure. Estimated stiffness was significantly lower in all directions at both radius and tibia. Particularly noteworthy was the finding that trabecular bone microarchitecture and stiffness were as severely affected in women with low BMD who had never had an adult low trauma fracture.

In our subjects, trabecular structure was as severely disrupted at the tibia as at the radius, and cortical structure was more severely affected at tibia than radius. In addition, we found correlations of borderline significance between fracture number and several cortical and trabecular parameters at the tibia, but not the radius. This contrasts with postmenopausal women with osteopenia, in whom radius but not tibia HR-pQCT measurements discriminated between those with and without fractures (14). It is also noteworthy because the tibia is a weight-bearing bone and one would predict that mechanical loading would result in relative sparing at that site (32, 33). The possibility of a defect in appropriate cortical and trabecular bone responses to weight bearing in women with IOP requires further exploration.

Several studies have reported that HR-pQCT parameters discriminate between postmenopausal women with and without fractures, whereas aBMD by DXA did not (14, 15, 17). Similarly, Melton *et al.* (18) reported that decreased vBMD, microstructure, and stiffness estimated by μFE of the radius are associated with forearm fracture in postmenopausal women. Our study confirms and extends these data by providing evidence of cortical and trabecular microarchitectural deterioration at both radius and tibia in premenopausal women with IOP, whether or not they have had a fracture.

To our knowledge, this is the first study to apply μFE to HR-pQCT scans from premenopausal women with IOP. μFE calculates apparent Young's moduli, an estimate of trabecular bone stiffness and an index of resistance to mechanical forces. Although a surrogate measure of stiffness, μFE analysis of a cube of trabecular bone has demonstrated excellent agreement with true biomechanical tests of bone specimens (34, 35) and μFE analysis of distal radius and tibia measurement sites, which include both trabecular and cortical bone. The latter have been shown to distinguish between postmenopausal women with and without fractures (17, 18). Because the technique we used analyzes only trabecular bone and does not include contributions from cortical bone, we may have underestimated differences in stiffness at the tibia, where cortical width and density were significantly higher in normal than affected women.

Other studies of young adults with unexplained fractures have yielded conflicting data on bone microarchitecture. Khosla *et al.* (12) found lower cancellous bone volume and cortical width in transiliac bone biopsies from young men and women with unexplained fractures. In contrast, in a retrospective study of biopsies from nine young women with low trauma fractures and 18 matched controls, we did not detect significant differences in cancellous bone volume, cortical width, Tb.N or Tb.Sp (13). Our prospective HR-pQCT study and retrospective biopsy results may differ because the biopsy study was smaller and had limited power to detect significant differences. In addition, we found rather weak correlations between structural parameters measured by HR-pQCT and by two-dimensional histomorphometry of transiliac bone biopsies in the same subjects (36). Thus, discrepancies between our previous and current results may be due to innate structural differences between the central unloaded iliac crest site and peripheral sites, both loaded (tibia) and unloaded (radius). However, although the inherent heterogeneity of the skeleton (37) raises concerns about generalizing our findings to other skeletal sites, we have also reported that HR-pQCT scans of the radius and tibia correlate strongly with central aBMD of the lumbar spine and proximal femur in the same subjects (36). In addition, we recently found significant correlations between elastic stiffness of the radius and tibia estimated by HR-pQCT-based μFE with that of the proximal femur and lumbar spine ($r^2 = 0.2–0.3$; $P < 0.01$), estimated from central QCT-based FE in the same subjects (38), suggesting that the estimated mechanical competence of the distal radius and tibia assessed by HR-pQCT predicts vertebral and femoral mechanical properties.

In postmenopausal women, particularly those over age 60, a fragility fracture or a low BMD measurement predicts future fractures (39). However, the clinical significance of fractures in young women is uncertain (40). It may be difficult to judge the level of trauma associated with the fracture. aBMD measurements may be within the expected range for age (Z score ≥ −2.0) in young women

with fractures, as they were for many of our fracture subjects. Although a premenopausal fracture is associated with a 33–74% increased risk of fracture after menopause (41, 42), few epidemiological data are available regarding the likelihood of future premenopausal bone loss or fractures. A small observational study of 16 young women with unexplained fractures managed with exercise, calcium, and vitamin D found that BMD improved slightly and no new fractures occurred (43). However, this may reflect the relative rarity of fractures in young *vs.* older women, regardless of aBMD measurements (1, 5).

The clinical significance of isolated low aBMD measurements in premenopausal women is even more uncertain. Some argue that in young, otherwise healthy women, a diagnosis of osteoporosis should be not made unless there has been a fracture (8, 44–46). One reason for the difficulty in interpreting low BMD measurements in premenopausal women is that DXA provides a two-dimensional areal measurement, does not take the thickness of the bone into consideration, and may underestimate true vBMD in smaller individuals (47). Both central (48) and peripheral QCT measure vBMD directly and thus may help ascertain whether a low aBMD measurement reflects a small bone of normal density or a true decrease in vBMD. It is perhaps because body size (and therefore bone size) influences DXA measurements that premenopausal women of small stature and thin habitus tend to have lower aBMD (7, 47, 49–53). However, our results suggest, at least in this small group of otherwise healthy women with low aBMD, that microarchitectural deterioration is as severe as in premenopausal women with fractures.

Another problem is that a single low BMD measurement provides no insight into whether it is simply due to low peak bone mass or to bone loss that has occurred previously or is ongoing—the pathophysiological mechanism common in postmenopausal women. Thus, some premenopausal women with low aBMD may have completely normal microarchitectural, dynamic, and material properties of bone. Others may have lost bone after having attained peak bone mass and, like similarly affected postmenopausal women, have microarchitectural abnormalities that compromise bone strength and increase fracture risk.

Finally, there are insufficient prospective data to assess the predictive value for fracture of a T score of less than −2.5 in premenopausal women. However, otherwise healthy, premenopausal women with low-energy wrist fractures have significantly lower forearm (54) as well as spine and hip (55) BMD than controls. Thus, low aBMD measurements in premenopausal women may mean that bone strength is compromised and represent a presymptomatic phase of IOP. Our results suggest that this is the case, at least in some women. Clearly, noninvasive tools to assess bone microarchitecture would be of great value in the management of such women.

Although our results delineate structural characteristics of bone, they do not speak to the pathogenesis of IOP in premenopausal women. In a previous study, we found lower follicular-phase serum estradiol levels and higher bone resorption markers in women with IOP, whereas serum IGF-I did not differ (52). Another study reported more frequent hypercalciuria (56, 57) and several suggest a genetic predisposition (51, 52, 56, 57). When recruitment is complete and biochemical analyses of archived serum and urine are available, it will be important to examine the relationships between the profound microstructural differences reported here and gonadal and calciotropic hormones, bone turnover markers, IGF-I, and cytokines.

This study has several limitations. Our younger subjects may not have reached peak bone mass. We may have misclassified fractures as low trauma when in fact they did not reflect abnormal fragility. Our sample size is too small to permit subgroup analyses by fracture type. Premenopausal women who have BMD measured or volunteered for this study may do so because of a family history of osteoporosis, thus biasing toward the finding of bone structural abnormalities. A small group of subjects and controls had serum 25-OHD concentrations under 20 ng/ml, a level currently considered to represent vitamin D deficiency. Although this may have influenced our findings, adjusting for serum 25-OHD and PTH did not affect the results. Because only cross-sectional data are available, we cannot determine whether observed abnormalities result from ongoing bone loss or past insults, now stabilized. Our μFE analyses examine a trabecular subvolume of the radius and tibia and thus may predict only trabecular rather than whole bone stiffness. Finally, assumptions of uniform bone mineralization are incorporated into μFE analyses.

Our study also has important strengths. To our knowledge, this is the largest case-control study of women with IOP and the only one to include noninvasive measurements of trabecular and cortical bone microarchitecture and trabecular stiffness. Both cases and controls were carefully characterized and common causes of secondary osteoporosis excluded by detailed clinical and biochemical evaluation.

In conclusion, we found significant microstructural differences in cortical and trabecular bone and estimated stiffness of the distal radius and the tibia between a group of premenopausal women with unexplained osteoporosis and a group of healthy women with normal aBMD.

Notably, the tibia, a weight-bearing bone, was as severely affected as the unloaded radius, and women with low aBMD who had not fractured were as severely affected as those included on the basis of one or more low trauma fractures. The finding that young women with low aBMD appear to have microarchitectural deterioration that is comparable to women who have sustained fractures is novel and could have implications for clinical management.

Acknowledgments

Address all correspondence and requests for reprints to: Adi Cohen M.D., M.H.S., Columbia University, College of Physicians & Surgeons, Department of Medicine, PH8-864, 630 West 168th Street, New York, New York 10032. E-mail: ac1044@columbia.edu.

This work was supported by National Institutes of Health Grants R01 AR049896 (E.S.), K23 AR054127 (A.C.), and R01 AR051376 (X.E.G.) and by the Thomas L. Kempner Jr. and Katheryn C. Patterson Foundation.

Disclosure Summary: The authors have nothing to disclose.

References

1. **Kanis JA** 2002 Diagnosis of osteoporosis and assessment of fracture risk. Lancet 359:1929–1936
2. **Kimmel DB, Recker RR, Gallagher JC, Vaswani AS, Aloia JF** 1990 A comparison of iliac bone histomorphometric data in post-menopausal osteoporotic and normal subjects. Bone Miner 11:217–235
3. **Parisien M, Cosman F, Mellish RW, Schnitzer M, Nieves J, Silverberg SJ, Shane E, Kimmel D, Recker RR, Bilezikian JP, Lindsay R, Dempster DW** 1995 Bone structure in postmenopausal hyperparathyroid, osteoporotic, and normal women. J Bone Miner Res 10:1393–1399
4. **Recker R, Lappe J, Davies KM, Heaney R** 2004 Bone remodeling increases substantially in the years after menopause and remains increased in older osteoporosis patients. J Bone Miner Res 19:1628–1633
5. **Hui SL, Slemenda CW, Johnston Jr CC** 1988 Age and bone mass as predictors of fracture in a prospective study. J Clin Invest 81:1804–1809
6. **Thompson PW, Taylor J, Dawson A** 2004 The annual incidence and seasonal variation of fractures of the distal radius in men and women over 25 years in Dorset, UK. Injury 35:462–466
7. **Gourlay ML, Brown SA** 2004 Clinical considerations in premenopausal osteoporosis. Arch Intern Med 164:603–614
8. **Lewiecki EM** 2004 Low bone mineral density in premenopausal women. South Med J 97:544–550
9. **Carter DR, Bouxsein ML, Marcus R** 1992 New approaches for interpreting projected bone densitometry data. J Bone Miner Res 7:137–145
10. **Katzman DK, Bachrach LK, Carter DR, Marcus R** 1991 Clinical and anthropometric correlates of bone mineral acquisition in healthy adolescent girls. J Clin Endocrinol Metab 73:1332–1339
11. **Heaney RP, Abrams S, Dawson-Hughes B, Looker A, Marcus R, Matkovic V, Weaver C** 2000 Peak bone mass. Osteoporos Int 11:985–1009
12. **Khosla S, Lufkin EG, Hodgson SF, Fitzpatrick LA, Melton 3rd LJ** 1994 Epidemiology and clinical features of osteoporosis in young individuals. Bone 15:551–555
13. **Donovan MA, Dempster D, Zhou H, McMahon DJ, Fleischer J, Shane E** 2005 Low bone formation in premenopausal women with idiopathic osteoporosis. J Clin Endocrinol Metab 90:3331–3336
14. **Boutroy S, Bouxsein ML, Munoz F, Delmas PD** 2005 *In vivo* assessment of trabecular bone microarchitecture by high-resolution peripheral quantitative computed tomography. J Clin Endocrinol Metab 90:6508–6515
15. **Sornay-Rendu E, Boutroy S, Munoz F, Delmas PD** 2007 Alterations of cortical and trabecular architecture are associated with fractures in postmenopausal women, partially independent of decreased BMD measured by DXA: the OFELY study. J Bone Miner Res 22:425–433
16. **Vico L, Zouch M, Amirouche A, Frère D, Laroche N, Koller B, Laib A, Thomas T, Alexandre C** 2008 High-resolution pQCT analysis at the distal radius and tibia discriminates patients with recent wrist and femoral neck fractures. J Bone Miner Res 23:1741–1750
17. **Boutroy S, Van Rietbergen B, Sornay-Rendu E, Munoz F, Bouxsein ML, Delmas PD** 2008 Finite element analysis based on in vivo HR-pQCT images of the distal radius is associated with wrist fracture in postmenopausal women. J Bone Miner Res 23:392–399
18. **Melton 3rd LJ, Riggs BL, van Lenthe GH, Achenbach SJ, Müller R, Bouxsein ML, Amin S, Atkinson EJ, Khosla S** 2007 Contribution of in vivo structural measurements and load/strength ratios to the determination of forearm fracture risk in postmenopausal women. J Bone Miner Res 22:1442–1448
19. **Laib A, Häuselmann HJ, Rüegsegger P** 1998 In vivo high resolution 3D-QCT of the human forearm. Technol Health Care 6:329–337
20. **Laib A, Rüegsegger P** 1999 Calibration of trabecular bone structure measurements of in vivo three-dimensional peripheral quantitative computed tomography with 28-microm-resolution microcomputed tomography. Bone 24:35–39
21. **Laib A, Hildebrand T, Häuselmann HJ, Rüegsegger P** 1997 Ridge number density: a new parameter for in vivo bone structure analysis. Bone 21:541–546
22. **Müller R, Hildebrand T, Häuselmann HJ, Rüegsegger P** 1996 In vivo reproducibility of three-dimensional structural properties of noninvasive bone biopsies using 3D-pQCT. J Bone Miner Res 11:1745–1750
23. **Melton 3rd LJ, Riggs BL, Keaveny TM, Achenbach SJ, Hoffmann PF, Camp JJ, Rouleau PA, Bouxsein ML, Amin S, Atkinson EJ, Robb RA, Khosla S** 2007 Structural determinants of vertebral fracture risk. J Bone Miner Res 22:1885–1892
24. **Riggs BL, Melton LJ, Robb RA, Camp JJ, Atkinson EJ, McDaniel L, Amin S, Rouleau PA, Khosla S** 2008 A population-based assessment of rates of bone loss at multiple skeletal sites: evidence for substantial trabecular bone loss in young adult women and men. J Bone Miner Res 23:205–214
25. **Laib A, Rüegsegger P** 1999 Comparison of structure extraction methods for in vivo trabecular bone measurements. Comput Med Imaging Graph 23:69–74
26. **Hildebrand T, Rüegsegger P** 1997 Quantification of bone microarchitecture with the structure model index. Comput Methods Biomech Biomed Engin 1:15–23
27. **MacNeil JA, Boyd SK** 2007 Accuracy of high-resolution peripheral quantitative computed tomography for measurement of bone quality. Med Eng Phys 29:1096–1105
28. **Zysset PK, Guo XE, Hoffler CE, Moore KE, Goldstein SA** 1999 Elastic modulus and hardness of cortical and trabecular bone lamellae measured by nanoindentation in the human femur. J Biomech 32:1005–1012
29. **Van Rietbergen B, Odgaard A, Kabel J, Huiskes R** 1996 Direct mechanics assessment of elastic symmetries and properties of trabecular bone architecture. J Biomech 29:1653–1657
30. **Hollister SJ, Brennan JM, Kikuchi N** 1994 A homogenization sampling procedure for calculating trabecular bone effective stiffness and tissue level stress. J Biomech 27:433–444
31. **Zhang XH, Liu XS, Vasilic B, Wehrli FW, Benito M, Rajapakse CS, Snyder PJ, Guo XE** 2008 In vivo microMRI-based finite element and morphological analyses of tibial trabecular bone in eugonadal and

hypogonadal men before and after testosterone treatment. J Bone Miner Res 23:1426–1434
32. **Judex S, Donahue LR, Rubin C** 2002 Genetic predisposition to low bone mass is paralleled by an enhanced sensitivity to signals anabolic to the skeleton. FASEB J 16:1280–1282
33. **Kuruvilla SJ, Fox SD, Cullen DM, Akhter MP** 2008 Site specific bone adaptation response to mechanical loading. J Musculoskelet Neuronal Interact 8:71–78
34. **Boyd SK, Müller R, Zernicke RF** 2002 Mechanical and architectural bone adaptation in early stage experimental osteoarthritis. J Bone Miner Res 17:687–694
35. **Ladd AJ, Kinney JH, Haupt DL, Goldstein SA** 1998 Finite-element modeling of trabecular bone: comparison with mechanical testing and determination of tissue modulus. J Orthop Res 16:622–628
36. **Cohen A, Dempster DW, Müller R, Guo XE, Nickolas TL, Liu XS, Zhang XH, Wirth AJ, van Lenthe GH, Kohler T, McMahon DJ, Zhou H, Rubin MR, Bilezikian JP, Lappe JM, Recker RR, Shane E** 20 May 2009 Assessment of trabecular and cortical architecture and mechanical competence of bone by high-resolution peripheral computed tomography: comparison with transilial bone biopsy. Osteoporos Int 10.1007/s00198-009-0945-7
37. **Hildebrand T, Laib A, Müller R, Dequeker J, Rüegsegger P** 1999 Direct three-dimensional morphometric analysis of human cancellous bone: microstructural data from spine, femur, iliac crest, and calcaneus. J Bone Miner Res 14:1167–1174
38. **Liu XS, Yin PT, Cohen A, Shane E, Lappe JM, Recker RR, Bilezikian JP, Guo XE** 2009 Relationships between stiffness of peripheral and central skeletal sites assessed by HR-pQCT and cQCT based finite element analyses. 55th Annual Meeting of the Orthopaedic Research Society, Las Vegas, NV, 2009
39. **Harvey N, Dennison E, Cooper C** 2008 Chapter 38. Epidemiology of osteoporotic fractures. Primer 7:198–203
40. **Cohen A, Shane E** 2008 Chapter 63. Premenopausal osteoporosis. Primer 7:289–293
41. **Hosmer WD, Genant HK, Browner WS** 2002 Fractures before menopause: a red flag for physicians. Osteoporos Int 13:337–341
42. **Torgerson DJ, Campbell MK, Thomas RE, Reid DM** 1996 Prediction of perimenopausal fractures by bone mineral density and other risk factors. J Bone Miner Res 11:293–297
43. **Peris P, Monegal A, Martínez MA, Moll C, Pons F, Guañabens N** 2007 Bone mineral density evolution in young premenopausal women with idiopathic osteoporosis. Clin Rheumatol 26:958–961
44. **Khan AA, Syed Z** 2004 Bone densitometry in premenopausal women: synthesis and review. J Clin Densitom 7:85–92
45. **Licata AA** 2000 "Does she or doesn't she . . . have osteoporosis?" The use and abuse of bone densitometry. Endocrine Practice 6:336–337
46. **Lindsay R** 1994 Bone mass measurement for premenopausal women. Osteoporos Int 4(Suppl 1):39–41
47. **Adams J, Bishop N** 2008 Chapter 29. DXA in adults and children. In: Rosen CJ, ed. Primer on the metabolic bone diseases and disorders of mineral metabolism. Washington, D.C.: American Society for Bone and Mineral Research; 152–158
48. **Glüer CC, Engelke K, Lang TF, Grampp S, Genant HK** 1995 Quantitative computed tomography (QCT) of the lumbar spine and appendicular skeleton. Eur J Radiol 20:173–178
49. **Bainbridge KE, Sowers M, Lin X, Harlow SD** 2004 Risk factors for low bone mineral density and the 6-year rate of bone loss among premenopausal and perimenopausal women. Osteoporos Int 15: 439–446
50. **Hawker GA, Jamal SA, Ridout R, Chase C** 2002 A clinical prediction rule to identify premenopausal women with low bone mass. Osteoporos Int 13:400–406
51. **Moreira Kulak CA, Schussheim DH, McMahon DJ, Kurland E, Silverberg SJ, Siris ES, Bilezikian JP, Shane E** 2000 Osteoporosis and low bone mass in premenopausal and perimenopausal women. Endocr Pract 6:296–304
52. **Rubin MR, Schussheim DH, Kulak CA, Kurland ES, Rosen CJ, Bilezikian JP, Shane E** 2005 Idiopathic osteoporosis in premenopausal women. Osteoporos Int 16:526–533
53. **Sowers MR, Shapiro B, Gilbraith MA, Jannausch M** 1990 Health and hormonal characteristics of premenopausal women with lower bone mass. Calcif Tissue Int 47:130–135
54. **Horowitz M, Wishart JM, Bochner M, Need AG, Chatterton BE, Nordin BE** 1988 Mineral density of bone in the forearm in premenopausal women with fractured wrists. BMJ 297:1314–1315
55. **Honkanen R, Tuppurainen M, Kroger H, Alhava E, Puntila E** 1997 Associations of early premenopausal fractures with subsequent fractures vary by sites and mechanisms of fractures. Calcif Tissue Int 60:327–331
56. **Peris P, Guañabens N, Martínez de Osaba MJ, Monegal A, Alvarez L, Pons F, Ros I, Cerdá D, Muñoz-Gómez J** 2002 Clinical characteristics and etiologic factors of premenopausal osteoporosis in a group of Spanish women. Semin Arthritis Rheum 32:64–70
57. **Peris P, Ruiz-Esquide V, Monegal A, Alvarez L, Martínez de Osaba MJ, Martínez-Ferrer A, Reyes R, Guañabens N** 2008 Idiopathic osteoporosis in premenopausal women. Clinical characteristics and bone remodelling abnormalities. Clin Exp Rheumatol 26:986–991